IFSCC 2025 full paper (IFSCC2025-940)

"Bionic Golden Ceramide EOP, beyond Skin Barrier Repairing"

Liu Ye[1]*, Chaowen Yang[1], Rui Huang[1], Yanmin Chen[1], Ping Zhao[2], Feifei Wang[3,4], Wenrou Su[3,4]

[1]Shenzhen Dieckmann Biotechnology Co., Ltd.; [2]School of Medicine and Chemical Engineering, Guangdong Pharmaceutical University.; [3] Yunnan Botanee Bio-technology Group Co., Ltd.; [4] Yunnan Characteristic Plant Extraction Laboratory, Yunnan Characteristic Plant Extraction Laboratory Co., Ltd.

---

1. Introduction

Ceramides（CERs）are found in almost all tissues of the human body, but the largest diversity of CERs is found in the human skin, more precisely in the stratum corneum (SC) of the epidermis[1]. CERs in the SC play a critical role in the formation and function of the permeability barrier [2-3]. There are various classes of CERs that derive from the combination of different types of sphingoid bases and fatty acids. Among them, EO CERs have unique structural features. EO CERs contain long-chain fatty acids with a terminal ω-hydroxyl group that is esterified predominantly with linoleic acid (LA). Based on their structure, EO ceramides are often referred to as ω-O-acylceramides or simply as acylceramides (acyl-Cers). AcylCers constitute approximately 10 weight % (roughly 7 mol %) of the SC Cers [4]. The presence of acylCer significantly contributes to the lamellar lipid organization in the SC [5-6]. Furthermore, acylCer is crucial for the formation of corneocyte lipid envelope (CLE)[7-8].

CER EOP is one representative class of acyl-Cers, which is believed to be very crucial for the molecular organization of SC lipids, since it can stabilize the lipid bilayer structure and strengthen the skin barrier. With unique acylceramide structure, CER EOP serves as a protein-bound ceramide through a pathway involving release of ω-OH CER and ester-linkage to the Glu residues of corneocyte envelope proteins. Traditional CER EOP with ultra-long carbon chain meets the drawbacks of poor solubility and unavailability, which greatly limited its widespread application in formulations. There is even no pure reference substance in the market. Consequently, there is no scientific data about CER EOP in skin care. All of these resulted in the fact that CER EOP has been seriously overlooked and underestimated. There is a great urgence for the development of CER EOP with commercial availability and in-depth research to elucidate its particular role in skin care.

The LC/APCI-MS method demonstrates that the most abundant CER species in SC have a carbon chain length between 40-52 carbon atoms and C46 has the highest abundance [9-10]. Hence, the development of novel CER EOP with bionic concept and commercial availability is of great interest.

This work aims to develop a novel C46 CER EOP with bionic concept and to address its supply shortage through the green industrilization process. On the other hand, this work intends to explore the skin benefits of the novel C46 CER EOP through in vitro cell test, particularly the direct efficacy comparion between CER EOP and tradditional CER (NP/AP) to elucitate that which has superior performance in skin barrier repairing. In addition, the exploration of new skin benefit of CER EOP was performed. Finally, the in vivo Raman spectroscopy was used to investigate its penetration ability and bioavailability.

2. Materials and Methods

2.1 Chemicals

The synthesis of CER EOP was achieved through a two-step reaction sequence. The initial transesterification occurred between glyceryl linoleate and 10-hydroxydecanoic acid under heated conditions (80°C). Upon completion of the reaction, the mixture was extracted with ethyl acetate and subsequently washed twice with deionized water. The organic phase was then dried over anhydrous sodium sulfate and concentrated under reduced pressure to yield intermediate **I.**

The subsequent condensation of intermediate **I** with phytosphingosine in the presence of coupling reagents with ethyl acetate as solvent delivered CER EOP: The reaction mixture of intermediate **I** with EDCI and SuOH was stirred at rt for 1 h before the addition of phytosphingosine and the reaction mixture continued to stir at rt for 12 h. After completion of the reaction, the mixture was quenched with deionized water and allowed to separate into distinct two phases. The organic layer was collected, washed with brine twice, dried, and concentrated under vacuum to obtain the crude product. Final purification was accomplished through ethanol recrystallization, yielding ceramide EOP as off-white solid with high purity.

2.2 Cell Viability Assay

HaCaT cells were seeded into 96-well plates at a density of 1×10^4 cells per well and incubated overnight in an incubator. After 24 hours, the supernatant was discarded, and 100 μL of medium containing different samples at different concentrations (CER EOP, CER 3B, CER 6) or blank medium was added to each well. Following further incubation for 24 hours, the medium was removed, and 100 μL of 3-(4,5-dimethylthiazol-2-yl)-2,5-diphenyltetrazolium bromide (MTT) solution was added to each well. The absorbance at 450 nm was measured, and cell viability was calculated as:

Cell viability (%) = OD570sample/OD570control × 100%

2.3 Evaluation of Anti-Inflammatory Efficacy of CER EOP and Comparion between CER EOP and CER NP (3 and 3B)

Seed B16 mouse melanoma cells at a density of 1×10⁴ cells/well in a 96-well plate, and allow them to adhere overnight in an incubator. After 24 hours, discard the supernatant, add 100 μL of different samples diluted with DMEM medium at different concentrations, and use DMEM medium without samples as the negative control group. Each group contains 3 replicate wells. Incubate the plate in an environment with 5% CO_2 at 37°C. Two hours after drug administration, add 10 μg/mL LPS to both the LPS model group and experimental groups, and continue co-incubation for 24 hours. After the reaction, collect 50 μL of cell supernatant and detect the expression of IL-6 gene in cells using an IL-6 ELISA kit.

2.4 Assessment of Endogenous Moisturizing Efficacy of CER EOP and Comparion between CER EOP and CER NP (3 and 3B)

Seed HaCat cells at a density of 1×10⁴ cells/well in a 96-well plate, and allow them to adhere overnight in an incubator. After 24 hours, discard the supernatant, add 100 μL of different samples diluted with DMEM medium at different concentrations, and use DMEM medium without samples as the negative control group. Each group contains 3 replicate wells. Incubate the plate in an environment with 5% CO_2 at 37°C. Two hours after drug administration, add 10 μg/mL LPS to both the LPS model group and experimental groups, and continue co-incubation for 24 hours. After the reaction, collect 50 μL of cell supernatant and detect the expression of AQP3 gene in cells using an AQP3 kit.

2.5 Assessment of Elastic Efficacy of CER EOP and Comparion between CER EOP and CER NP (3 and 3B)

Take 2 mL of 2 mg/mL elastase solution, add different samples at different concentrations, vortex thoroughly to mix, and incubate on a shaker at 37°C and 400 r/min for 20 min. Immediately add 5 mL of 0.5 mol/L phosphate buffer (pH 6.0), vortex again to mix. Transfer an appropriate amount of the mixed solution into 2 mL centrifuge tubes, centrifuge at 9391×g for 10 min. Precisely pipette 200 μL of the supernatant into a 96-well plate, measure the absorbance at 495 nm using a microplate reader, and perform spectroscopic scanning across 400–800 nm simultaneously.Each experimental condition was performed in triplicate to ensure data reliability.

The percentage inhibition of elastase activity was calculated by comparing the absorbance values between different control groups. Specifically, the inhibition rate was derived from the difference between sample-treated reactions and enzyme-only controls, normalised against the background absorbance of substrate alone. This calculation method accounts for any potential interference from the sample matrix and provides an accurate measure of elastase inhibition.

Inhibition Rate (%) = [1 − (An − An′) / (A0 − A0′)] × 100

A0 = Absorbance with enzyme;

A0′ = Absorbance with substrate only;

An = Absorbance with test sample;

An′ = Absorbance with test sample and substrate.

2.6 Skin Permeation Assay

The skin permeation behavior of CER EOP was evaluated in vivo using a LabRAM Soleil high-resolution confocal Raman microscope (Horiba Scientific, Japan). A 30-year-old healthy female volunteer was recruited for the study, with the volar forearm selected as the test site (1 cm^2 area). Before measurement, the skin surface was gently cleansed with purified water, followed by a 30-min acclimatisation period in a controlled environment (25±1°C, 50±5% relative humidity). Skin barrier integrity was confirmed using a corneometer. After uniform application of CER EOP, Raman spectra were acquired at predetermined time points (0 h, 0.5 h, 1 h, 2 h, and 4 h). For each time point, five distinct locations within the test area were measured in triplicate to ensure data reproducibility. The measurements were performed using a 72 μW laser with 0.5 s integration time per point. Depth profiling was conducted in X-Z scanning mode with a step size of 10 μm, covering an area of 20 μm (lateral) × 120 μm (depth). The total acquisition time for each scan was maintained within 3 min to minimise motion artifacts. Spectral data were processed using Labspec 6.0 software. Baseline correction was performed using adaptive iteratively reweighted least squares (airPLS), followed by noise reduction via Savitzky-Golay filtering. Characteristic vibrational peaks of CER EOP were analyzed to determine peak intensity, area, and full width at half maximum (FWHM). The relative permeation rate (%) was calculated as:

Relative Permeation (%)=(Raman intensity on skin surface ÷ Raman intensity in skin)×100

All procedures were conducted in compliance with ethical guidelines, with written informed consent obtained from the participant before the study.

3. Results

3.1 Cell Viability

Based on HaCat cell test, the results showed that when the concentration of CER EOP was 0.0625 mM, cell viability reached 114.7%, and at a concentration of 0.5 mM, cell viability reached 122.3%, exhibiting a significant effect in promoting cell proliferation and demonstrating potential for tissue repair. Meanwhile, within a concentration range up to 1 mM, no cytotoxicity was observed, indicating good biological safety (**Figure 1a**). In comporsion, the results of the cell proliferation activity assay for CER NP(3B) and CER AP(6) are also listed in the Figure 1b and 1c. Both CER EOP and ceramide NP/AP exhibit good capabilities for cell repair and tissue repair.

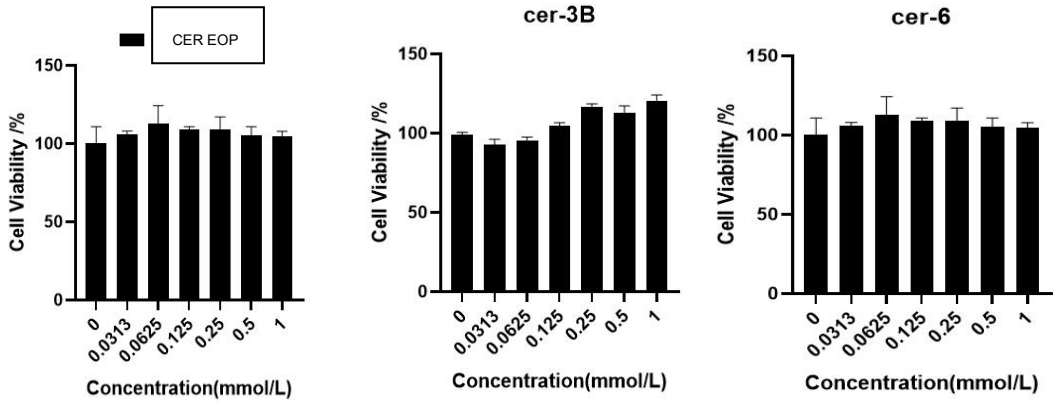

(a) (b) (c)

Figure 1 Cell viability of different CER samples

3.2 Evaluation of Anti-Inflammatory Efficacy

Based on B16 cell test, the results showed that LPS successfully induced an inflammatory model in B16 cells, with the expression of the inflammatory cytokine IL-6 in model cells up to 23.14 times than that of the control group. CER EOP exhibited excellent inhibitory effects on IL-6 cytokine expression. At concentrations of 0.1, 0.2, 0.4, 0.8, and 1.00 mM, the expression levels of the IL-6 factor were 12.37, 6.15, 3.04, 1.31, and 0.65 fold compared to the control group, respectively (**Figure 2a**). Compared to the LPS model group, the inhibition rate reached up to 46.54%, 73.42%, 86.86%, 94.30%, and 97.19%, respectively. Therefore, CER EOP demonstrates good anti-inflammatory effects and is expected to promote the repair of inflammation-damaged skin.

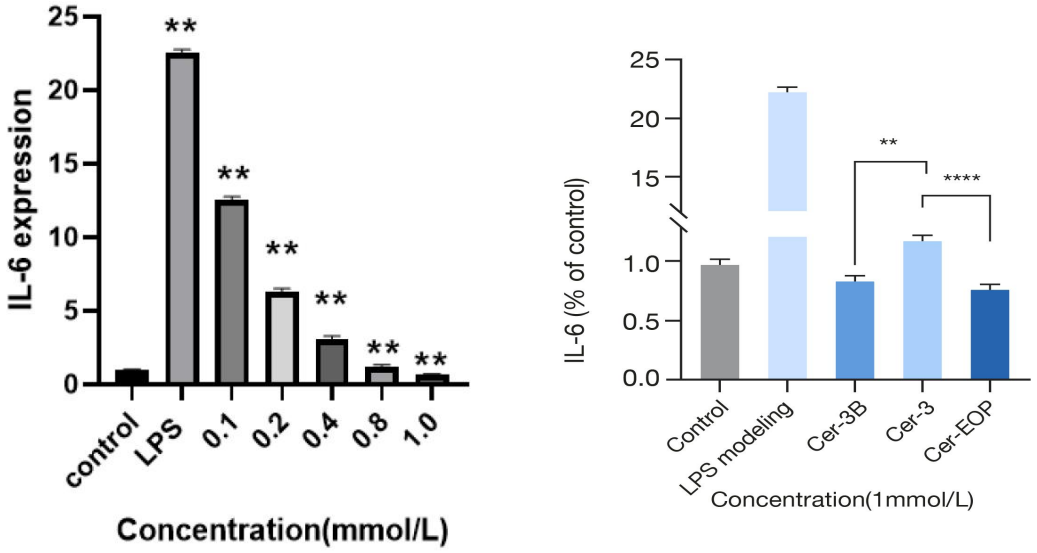

(a) (b)

Figure 2 Inhibition of the IL-6 inflammatory cytokine with CER samples

Interestingly, when the direct comparion between CER EOP and CER NP (3 and 3B) were tested, the results showed that although all of them could effectively inhibit the expression of the IL-6 inflammatory cytokine at concentration of 1.00 mM, the CER EOP exhibited the most significant inhibitory effect on IL-6 (**Figure 2b**).

3.3 Assessment of Endogenous Moisturizing Efficacy

The results showed that the addition of CER EOP effectively increased the expression level of AQP3 water channel protein in a concentration-dependent manner. At sample concentrations of 0.4, 0.8, and 1.6 mM, the AQP3 expression levels were elevated 1.12-fold, 1.33-fold, and 1.47-fold than those of the vehicle control group, respectively (**Figure 3a**).

When comparing the moisturizing efficacy of CER EOP and CER NP (3 and 3B) at concentration of 1 mM, the results disclosed that all tested samples showed a significant increase in the content of aquaproin 3, while CER EOP demonstrated the highest enhancement rate (**Figure 3b**).

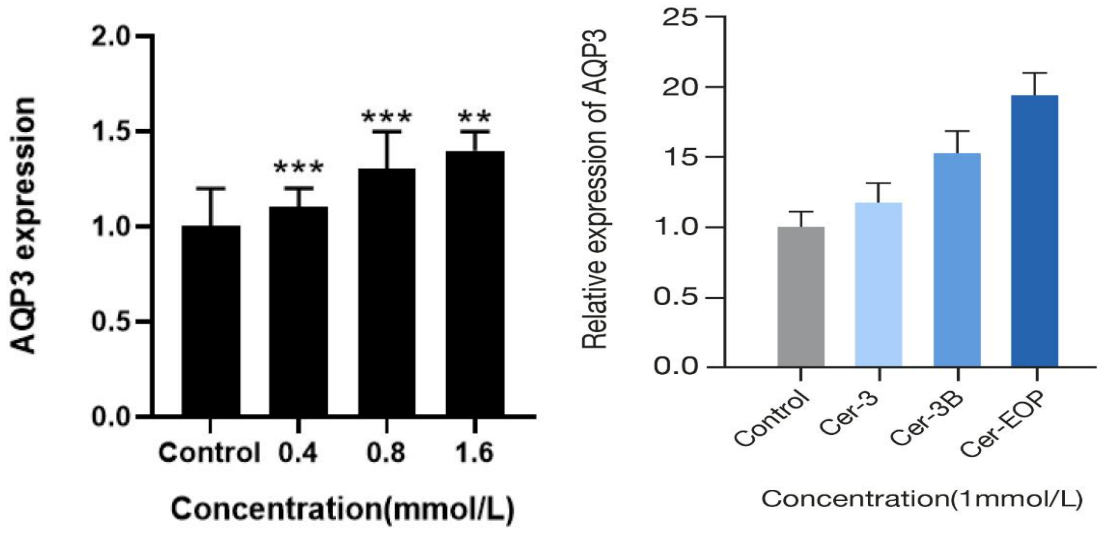

(a) (b)

Figure 3 Increment of AQP3 with different CER samples

3.4 Assessment of Elastic Efficacy

The results showed that CER EOP remarkbly increased the elastase inhibition rate in a concentration-dependent manner. At concentrations of 0.4, 0.8, and 1.0 mM, the inhibition rates were enhanced by 18.21%, 22.07%, and 25.37% (**Figure 4a**), respectively, indicating that it can inhibit elastase expression, protect elastin, and maintain or enhance skin elasticity.

When compared with Ceramide 3, Ceramide 3B, CER EOP was significantly superior in elastase inhibition ability at a concentration of 1 mmol/L, exhibiting the best inhibitory effect on elastase (**Figure 4b**).

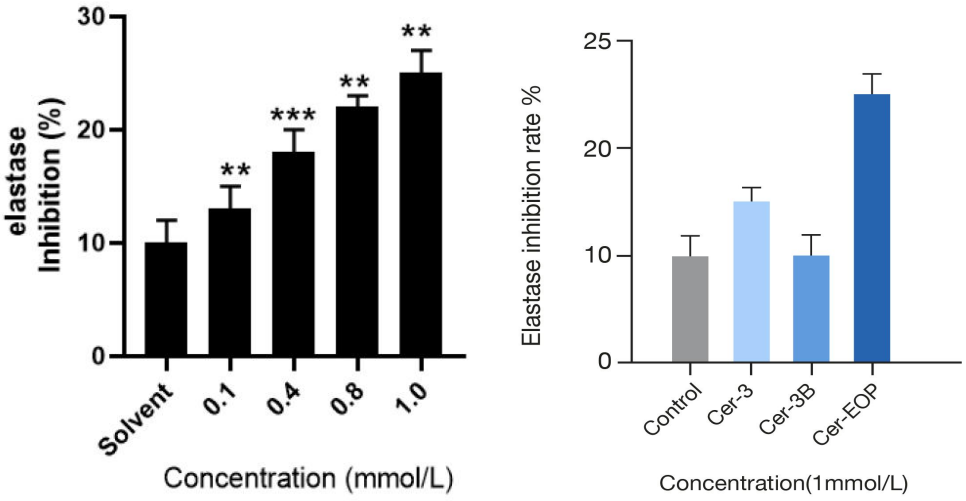

(a) (b)

Figure 4 Enhancement of elastase inhibition with different CER samples

3.5 Skin Permeation Assay

The intrinsic Raman spectrum of human in vivo skin revealed characteristic vibrational peaks at 943 cm^{-1}, 1275 cm^{-1}, 1455 cm^{-1}, 1655 cm^{-1}, 2846 cm^{-1}, 2883 cm^{-1}, 2934 cm^{-1}, and 3226 cm^{-1} (**Figure 5**). These spectral signatures correspond to key biomolecular components, including amino acids，nucleic acids, structural proteins, and intercellular lipids.

This comprehensive spectral analysis established a baseline for assessing skin biochemistry prior to CER EOP application. Subsequent Raman mapping further confirmed the penetration kinetics of CER EOP, demonstrating its progressive accumulation in the stratum corneum over time. The distinct spectral fingerprints of both untreated skin and CER EOP enabled precise differentiation between endogenous skin components and the applied formulation, providing critical insights into its transdermal delivery efficiency.

Building on this foundation, analysis of CER EOP demonstrated distinct characteristic peaks at 635-3082 cm^{-1} (**Figure 6**), confirming its structural identity through specific molecular vibrational modes. Depth-resolved Raman imaging (**Figure 7**) revealed the compound's dynamic penetration kinetics. While initial measurements at 0 h showed no ceramide EOP in the stratum corneum, penetration became detectable at 0.5 h (1.45%) and progressively increased to 3.15% (1 h), 5.72% (2 h), and 7.19% (4 h) (Table 1), with clear visualization of distribution patterns in Figure 7. This time-dependent permeation through the stratum corneum into the viable epidermis provides compelling in vivo evidence for CER EOP's transdermal delivery potential, supported by the molecular specificity of Raman spectroscopy in distinguishing exogenous compounds from endogenous skin components.

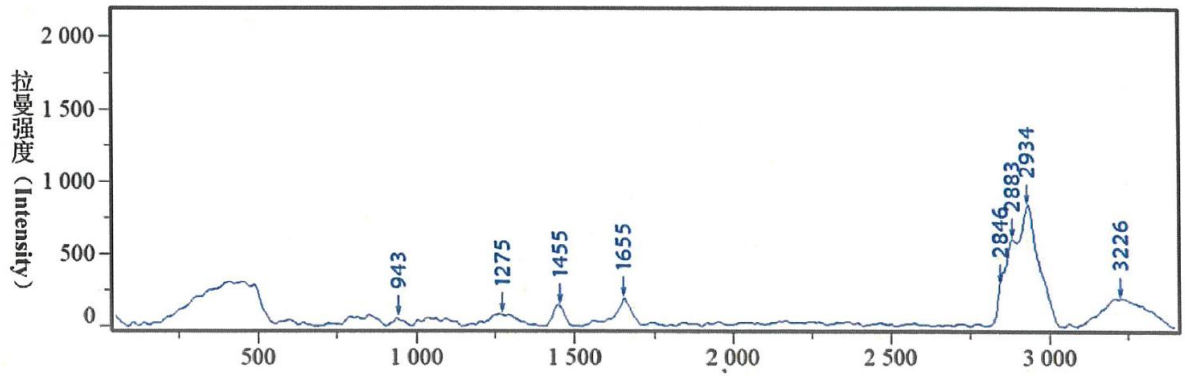

Figure 5 Raman spectrum of human in vivo skin

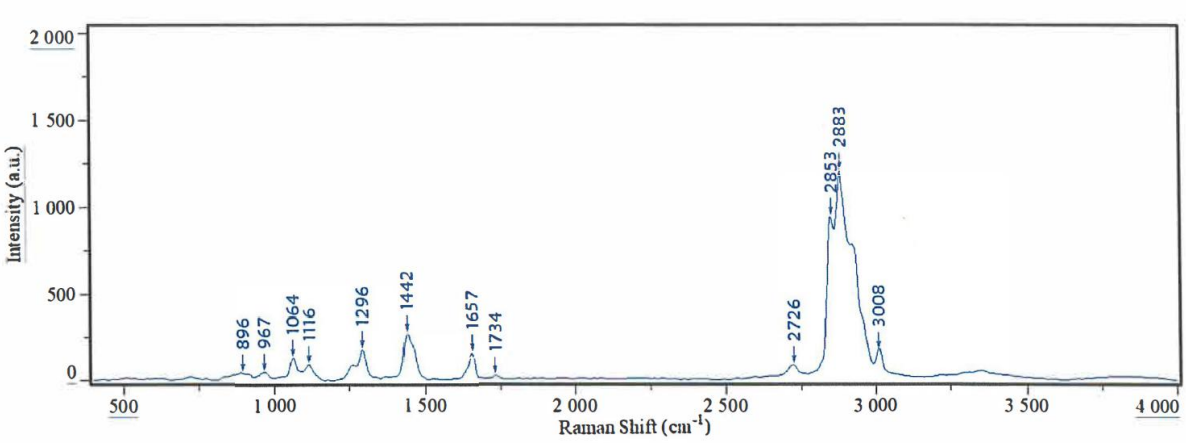

Figure 6 Raman spectrum of CER EOP

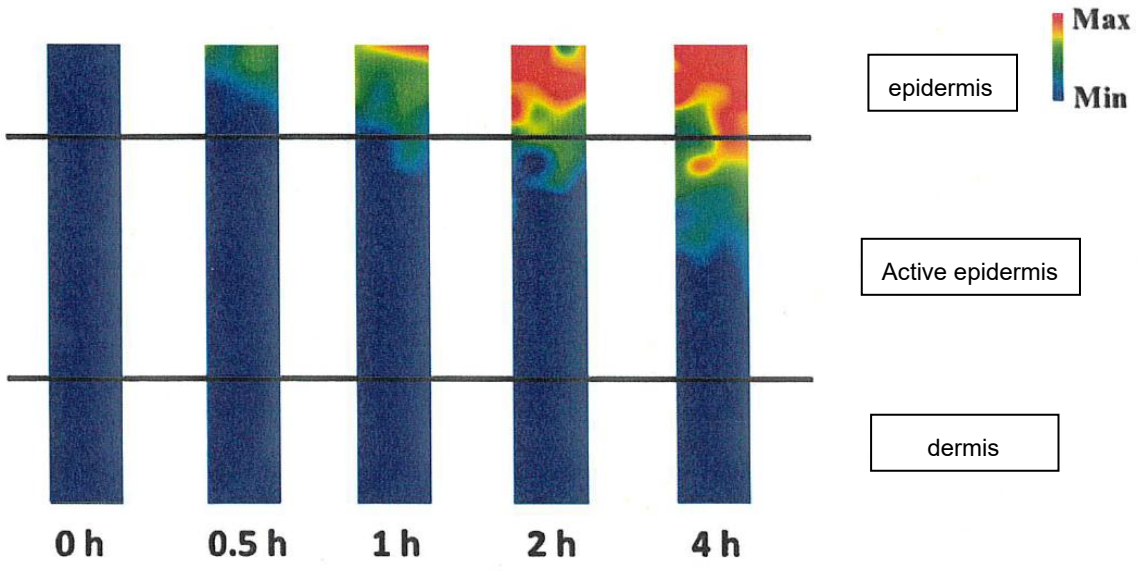

Figure 7 Depth-resolved Raman imaging of CER EOP

Table 1. CER EOP penetration depth

CER EOP use time (h)	Maximum depth of penetration (μm)
0.5	15
1	25

2	40
4	60

4. Discussion

According to carbon chain length distribution principle of ceramide in human skin, a bionic C46 CER EOP was designed. The great challenge of supply shortage of ultra-long chain CER EOP was also successfully addressed, since a large-scale green preparation process of C46 CER EOP was achieved. Notably, the product derives from bio-based raw materials, which meets the requirement for sustainable development and clean beauty. Cell viability test demonstrated that bionic CER EOP has similar high safety concentration as CER NP/AP, which indicates that CER EOP, as endogenous lipid, has excellent biological safety. Assessment of anti-inflammatory efficacy and moisturizing efficacy of CER EOP revealed that, comparted to CER NP(3 and 3B), it has better efficacy in inhibiting the expression of interleukin-6 inflammatory factor and improving the expression levels of AQP3. The excellent performance in skin barrier repairing observed for bionic CER EOP might resides dominantly in its ability to stabilize the lipid bilayer structure to form tight lamellar lipid organization. Beyond well-known skin barrier repairing ability, the new skin benefit of CER EOP to improve skin elasticity was firstly identified. It is worthy of in-depth research to explore underlying relationship between CER EOP and elastase inhibiton. In vivo Raman spectroscopy experiment clearly demonstrated that bionic CER EOP has good penetration ability into epidermis, which might result from its unique structure. This observation is indicative of good bioavailability for this new functional ingredient. The metabolic process of CER EOP in the skin, as well as whether CER EOP itself or its metabolites can enter the dermis and exert their effects, still requires further research.

5. Conclusion

In summary, we have developed a novel bionic CER EOP, as well as its green industrilization process from biobased materials. Breakthroughs in technology will greatly promote the high-content addition of CER EOP in the formula. Many cell tests in vitro unvealed that this unique CER EOP has superior performace in skin barrier repairing efficacy than traditional CER NP(3 and 3B), which will provide a scientific basis for formulators' choices. The discovery of new anti-aging efficacy breaks the traditional understanding of the functions of ceramide, which will spurr the continuous exploration of other high-levels efficacy of ceramide in skin care. Raman spectroscopy in vivo test implys that CER EOP can rapidly penetrate into the skin's stratum corneum to mediate barrier repair. Collectively, our research confirms that C46 CER EOP is an outstanding skincare active. The powerful skin benefits are probably related to its unique structure, and the underlying association needs further investigation.

【1】 Kihara A, Synthesis and degradation pathways, functions, and pathology of ceramides and epidermal acylceramides. *Prog. Lipid. Res.* **2016**, 63, 50–69.

【2】 Elias PM, Menon GK. Structural and lipid biochemical correlates of the epidermal permeability barrier. *Adv. Lipid. Res.* **1991**, 24, 1-26.

【3】 Uchida, Y.; Holleran,W.M. Omega-O-acylceramide, a lipid essential for mammalian survival. *J. Dermatol. Sci.* **2008**, 51, 77–87.

【4】 Masukawa Y, Narita H, Sato H, Naoe A, Kondo N, Sugai Y, et al. Comprehensive quantification of ceramide species in human stratum corneum. *J Lipid Res*. **2009**, 50, 1708-1719.

【5】 Bouwstra, J.A.; Gooris, G.S.; Dubbelaar, F.E.; Weerheim, A.M.; Ijzerman, A.P.; Ponec, M. Role of ceramide 1 in the molecular organization of the stratum corneum lipids. J. Lipid Res. **1998**, 39, 186–196.

【6】 Opálka L, Kováčik A, Maixner J, Vávrová K. Omega-O-Acylceramides in Skin Lipid Membranes: Effects of Concentration, Sphingoid Base, and Model Complexity on Microstructure and Permeability. *Langmuir*. **2016**, 32, 12894-12904.

【7】 Elias, P.M.; Gruber, R.; Crumrine, D.; Menon, G.; Williams, M.L.; Wakefield, J.S.; Holleran, W.M.; Uchida, Y. Formation and functions of the corneocyte lipid envelope (CLE). *Biochim. Biophys. Acta* **2014**, 1841, 314–318.

【8】 Fujii, M. The Pathogenic and Therapeutic Implications of Ceramide Abnormalities in Atopic Dermatitis. Cells **2021**, 10, 2386.

【9】 van Smeden, J.; Boiten, W.A.; Hankemeier, T.; Rissmann, R.; Bouwstra, J.A.; Vreeken, R.J. Combined LC/MS-platform for analysis of all major stratum corneum lipids, and the profiling of skin substitutes. *Biochim. Biophys. Acta* **2014**, 1841, 70–79.

【10】 t'Kindt, R.; Jorge, L.; Dumont, E.; Couturon, P.; David, F.; Sandra, P.; Sandra, K. Profiling and characterizing skin ceramides using reversed-phase liquid chromatography-quadrupole time-of-flight mass spectrometry. *Anal. Chem.* **2012**, 84, 403–411.